

# Electronic Structure of 1,3,5,7-Cyclooctatetraene Chemisorbed on Si(001)-2×1 at 300 K Studied by PES, NEXAFS, and Resonant Valence Band Spectroscopy

F. Rochet,\* F. Bournel, J.-J. Gallet, and G. Dufour

Laboratoire de Chimie Physique – Matière et Rayonnement, UMR 7614, Université P. et M. Curie, 11 rue Pierre et Marie Curie, F-75231 Paris Cedex 05, France

L. Lozzi

INFN, Dipartimento di Fisica, Università dell'Aquila, Via Vetoio, I-67010 Coppito, L'Aquila, Italy

F. Sirotti

Laboratoire pour L'Utilisation du Rayonnement Electromagnétique, Centre Universitaire Paris-Sud, Bâtiment 209D, B. P. 34, F-91898 Orsay Cedex, France

Received: October 10, 2001; In Final Form: January 29, 2002

The electronic structure of 1,3,5,7-cyclooctatetraene, an antiaromatic molecule, adsorbed on Si(001)-2×1 at 300 K has been investigated by a combination of core-level spectroscopies using synchrotron radiation. Si 2p and C 1s photoemission spectroscopy (PES) are used to follow the reaction of silicon surface states and the formation of Si–C bonds. C 1s near-edge X-ray absorption fine structure (NEXAFS) spectroscopy shows that p bonds survive after chemisorption. The orientational order of the free p bonds is deduced from the angular dependence of the NEXAFS spectra; performed on a single domain (vicinal) surface, this study indicates that multiple adsorption geometries are actually adopted by the chemisorbed molecules. Finally, resonant valence band spectroscopy gives the binding energy position of the occupied p band of the chemisorbates, information that may be useful for the interpretation of scanning tunneling microscopy images.

## I. Introduction

In the footsteps of Yoshinobu and co-workers,<sup>1</sup> who discovered that ethylene bonds undissociatively (at 300 K) to the Si<sub>2</sub> dimers of Si(001) via a cycloaddition reaction, many surface science groups have undertaken a systematic (and rather fundamental) study of the chemisorption of  $\pi$ -bonded organic molecules on this technologically important surface. In addition to ethylene, the researchers' attention has been attracted by the adsorption of poly-enes, essentially dienes, either conjugated<sup>2,3</sup> (to study a possible Diels–Alder addition mechanism) or nonconjugated,<sup>4–7</sup> and aromatics, essentially benzene (see e.g., ref 8). A review on the adsorption of such molecules, principally focused on scanning tunneling microscopy (STM) experiments, has recently been written by Robert Wolkow.<sup>9</sup>

1,3,5,7-Cyclooctatetraene (C<sub>8</sub>H<sub>8</sub>, in short COT) is a molecule whose adsorption on the Si(001) surface is also worth studying because of its particular electronic structure and conformation.<sup>10</sup> This is an antiaromatic molecule which adopts a “tub” shape (the symmetry is  $D_{2d}$ , see Figure 1), leading to four independent  $\pi$  systems. The planar forms of the molecule, of  $D_{4h}$  and  $D_{8h}$  symmetry, are transition states in the fast interconversion between the four  $D_{2d}$  stable conformations (note that on the singlet ground-state potential energy surface  $D_{4h}$  is calculated to be 0.73 eV higher in energy than  $D_{2d}$  in a MP2–CASSCF calculation<sup>11</sup> and 0.45 eV in a density functional calculation<sup>12</sup>). However, both the mono- and dianions are planar in solution<sup>13</sup> (note that the dianion is aromatic).

Because of the particular electronic structure of the molecule, multiple bonding configurations on the Si surface are expected. If one assumes that the molecule maintains its  $D_{2d}$  symmetry while approaching the surface, a single [2+2] cycloaddition<sup>14</sup> of one alkene group with one Si<sub>2</sub> dimer has to be envisaged, leading to a “[2+2]” adduct (a conjugated triene is represented in Figure 1). Given that the distance of  $\sim 3.15$  Å,<sup>12</sup> which separates the C=C groups, at the two opposite ends of the free molecule, is close to the surface lattice spacing along a  $\langle 110 \rangle$  direction (3.85 Å), a bridging geometry can also be drawn, where two opposite alkene groups react with two adjacent silicon dimers of the same row (the “dual [2+2]” geometry given in Figure 1).<sup>15</sup> Alternately, if the molecule adopts a planar geometry in the immediate vicinity of the surface (for example via a charge transfer from the substrate), then a Diels–Alder adduct (denoted “[4+2]” in Figure 1) can be formed by reaction with one Si<sub>2</sub> dimer (see refs 2 and 3). If two adjacent Si<sub>2</sub> dimers are involved, then a cross-dimer bridging geometry (denoted “dual [4+2]” in Figure 1) is obtained.<sup>16</sup>

Experimentally, the adsorption of COT was studied by Hovis and Hamers<sup>17</sup> with infrared (IR) spectroscopy and STM. IR spectroscopy performed on a single domain vicinal surface demonstrated that the molecule adsorbs nondissociatively on the surface, leaving intact (unreacted) alkene groups. Although the radiation polarization could be oriented with respect to the dimer row direction, no information on the molecule orientational order could be obtained. The STM images taken at a sample bias  $V_b$  of  $-2.2$  V pointed to the formation of one majority adduct (95% of the adsorption sites, according to ref 17), whose “footprint” is elongated along the dimer row (the

\* To whom correspondence should be addressed. E-mail: roch@ccr.jussieu.fr. Fax: (+33) 1 44 27 62 26.

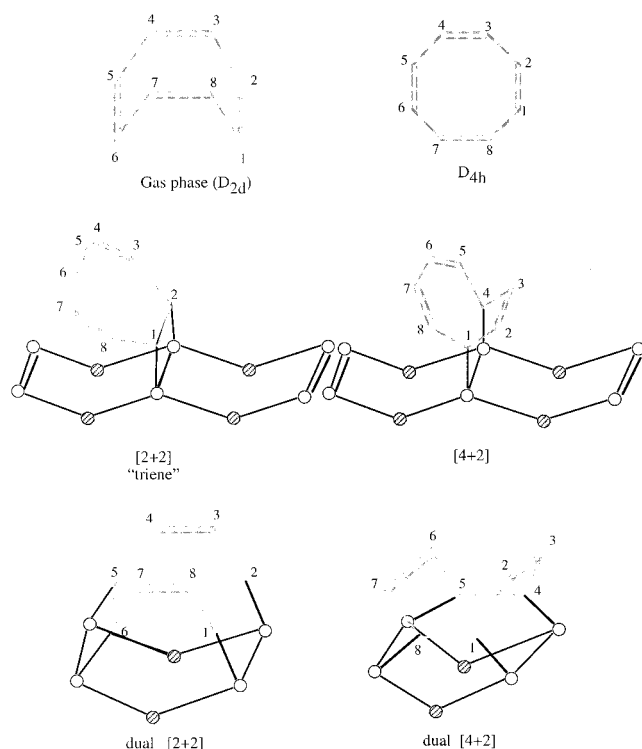


**Figure 1.** Possible schematic bonding geometries of COT on Si(001)- $2\times 1$ . Circles designate surface silicon atoms (white circles, surface dimers; hatched circles, second plane silicons). The carbon-carbon bonds are drawn in gray (H atoms are not represented). In the gas phase ( $D_{2d}$  symmetry), the distances C1-C2, C2-C3, C2-C5, and C1-C4 are 1.35, 1.47, 3.15, and 3.26 Å; for the  $D_{4h}$  transient, C1-C2 and C2-C3 remain practically unchanged, whereas C1-C4 increases to  $\sim 3.4$  Å (ref 12). Note that in a [2+2] (respectively [4+2]) cycloaddition carbons labeled C1 and C2 (respectively C1 and C4) form two  $\sigma$  bonds with the silicon dimers.

minority species footprint exhibits two parallel bars aligned with the dimer row direction). At saturation, the images showed that all dimers site are reacted; that is, there is one chemisorbed per two dimer sites. The separation between the molecule is 7.7 Å, i.e., twice the distance between two adjacent  $\text{Si}_2$  dimers pertaining to the same row. Local ( $2\times 2$ ) or  $c(4\times 2)$  ordering is observed. Because of the adsorbate footprint (the majority species has two mirror planes, parallel to (110) and ( $\bar{1}\bar{1}0$ )), only "bridge" configurations (the adsorption site consists of two adjacent  $\text{Si}_2$  dimers), like those denoted "dual [2+2]" and "dual [4+2]", in Figure 1, have been retained by Hovis and Hamers. Of the two considered geometries, a density functional cluster calculation showed that the "dual [2+2]" configuration has the lowest energy and, hence, corresponds to the majority species. However, reexamining the images and interpretations of ref 17, Wolkow suggests that the majority species (elongated along the dimer row direction) would rather correspond to the "dual [4+2]" geometry, whereas the 5% minority species would adopt the "dual [2+2]" geometry.<sup>9</sup>

It seems indeed very plausible that this molecule displays a rich variety of bonding geometries. In a successive paper,<sup>18</sup> Padowitz and Hamers have examined the influence of sample bias  $V_b$  on molecular imaging: although at  $V_b = -3$  V an image of a given area is indicative of only one adsorbed species (as in ref 17), surprisingly, an image of the same scanned area taken at  $-1.0$  V showed the presence of two species (the statistical distribution of the different species is not given). The authors proposed that the molecule could be also attached to the surface by only one C=C group, leaving three intact C=C forming a

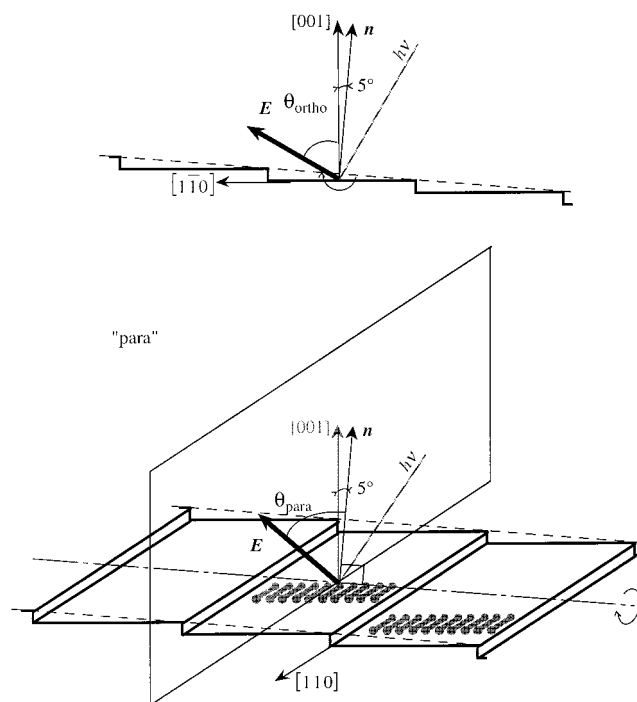


**Figure 2.** Geometry of the NEXAFS experiment carried out on a Si(001) vicinal surface. The small dumbbells (in gray) represent schematically the  $\text{Si}_2$  surface dimers.

planar conjugated triene ("[2+2]" in Figure 1). However, the reason, for two different adducts, there is one footprint at high bias and two footprints at low bias is not given.

The aim of the present work is to add new experimental data provided by a combination of core-electron spectroscopies to the file of COT chemisorption on Si(001). First, the conditions leading to saturation coverage are determined by C 1s photoemission spectroscopy (PES) (at  $h\nu = 340$  eV) and Si 2p PES (in surface sensitive conditions at  $h\nu = 145$  eV, so that the intensity of the "surface state" resulting from silicon dimerization can be measured). Second, a C 1s NEXAFS spectroscopy study is carried out. NEXAFS spectroscopy, which probes the carbon unfilled states of p symmetry, is able to detect the presence of specific bonds in the molecules (e.g.,  $\pi$  bonds via the observation of a  $1s \rightarrow \pi^*$  resonance at a photon energy close to the C 1s binding energy).<sup>19</sup> NEXAFS gives also information on the orientation of the nonoccupied p orbitals. The dipole absorption from a 1s level has a characteristic  $\cos^2(\delta)$  dependence, where  $\delta$  is the angle between the p orbital axis and the polarization vector  $E$ .<sup>20</sup> To take a full advantage of the capability of this spectroscopy to determine  $\pi$  bond orientations, the COT molecule needs to be deposited on a single-domain vicinal surface. It is well-known that on-axis surfaces consist of  $2\times 1$  and  $1\times 2$  domains in equal quantities, with the dimer rows of one domain running perpendicular to the dimer rows of the other. On the other hand, a vicinal Si(001) surface, cut by more than  $2^\circ$  off [001] axis, toward ( $\bar{1}\bar{1}0$ ), here the surface is misaligned by  $5^\circ$ , forms a regular array of bi-steps and single  $2\times 1$  reconstructed surface domain terraces. Then the electric vector  $E$  of the linearly polarized synchrotron radiation can be placed in a plane parallel or orthogonal to the silicon dimer axis (see Figure 2). Vicinal surfaces are often used to obtain single domain surfaces,<sup>6,8,17</sup> although there are some drawbacks: with respect to an on-axis surface, they present a higher density of steps, to which the adsorbate can bond with a geometry different from that of the terrace (this will be discussed in section III.C).<sup>21</sup> Finally, resonant valence band spectroscopy at the

photon energy of the C 1s  $\rightarrow \pi^*$  NEXAFS transition is used to determine the binding energy position of the  $\pi$  level(s), an information that may prove useful for the interpretation of STM experiments.

## II. Experimental Section

### A. Clean Surface Preparation and Exposure to the Gas.

Si samples are prepared in a ultrahigh-vacuum (UHV) chamber whose base pressure is  $\sim 10^{-10}$  Torr. The phosphorus-doped silicon wafers (of resistivity 0.002–0.005  $\Omega\text{cm}$ ) are heated by Joule effect (temperature measurements are made by infrared pyrometry). They are cleaned of their silica protective layer by heating at  $\sim 1520$  K, to minimize SiC contamination.<sup>22</sup> The surface cleanliness is checked by the intensity of the Si 2p core-level surface state, by a survey of the C 1s region, and by the sharpness of the low energy electron diffraction (LEED) patterns characteristic of a two-domain (on-axis (001) surface) or of a single-domain (vicinal surface)  $2\times 1$  pattern.

Then the silicon surface is exposed at 300 K to COT, purified by several freeze–pump–thaw cycles, under a pressure of  $10^{-8}$  mbar (measured with an ionization gauge whose reading is not corrected) for durations up to 450 s. Multilayers of solid COT are also prepared by condensation of the molecules on the substrate maintained at 90 K (under a pressure of  $5 \times 10^{-8}$  mbar, for 1800 s).

**B. Photoemission Spectroscopy (PES).** Valence bands and core-level (Si 2p, C 1s) spectra are measured with monochromatic synchrotron radiation delivered by the linear undulator of beam line SU7 of the SuperACO storage ring (Orsay). A hemispherical electron energy analyzer is used, having an angle acceptance of ca.  $\pm 8^\circ$ . The angle between the direction of light and the analyzer axis is constant and equal to  $44^\circ$ . The plane defined by light incidence and electron emission is parallel to a {110} plane of the substrate. The polar angle  $\theta$  of the electric field  $E$  and the emission angle  $\alpha$  of the detected photoelectrons are measured from the normal to the optical plane  $n$ , coincident with the [001] direction for the on-axis surface.

Photons of energy  $h\nu = 145$  eV are used to excite the Si 2p core-level of binding energy (BE) around 99–100 eV, in conditions of maximum surface sensitivity: for photoelectrons of kinetic energy around  $\sim 45$  eV, an escape depth of about 3.3 Å is estimated.<sup>23</sup> The C 1s spectra are recorded at  $h\nu = 340$  eV. Resonant valence bands are measured around the C 1s edge ( $h\nu = 285$  eV). The analyzer energy resolution is 150 meV for C 1s and Si 2p core levels and 300 meV for valence bands. The photon bandwidth is ca. 290 meV at  $h\nu = 145$  eV and ca. 510 meV at  $h\nu = 340$  eV.

To improve the resolution of the various components that contribute to the Si 2p spectra, the procedure given in ref 24 is followed. The background is first subtracted. Then the low  $j$  component of the Si  $2p_{1/2,3/2}$  doublet is removed, mathematically (assuming identical shapes for the two components), with a branching ratio  $2p_{1/2}:2p_{3/2}$  of 0.5 (the statistical ratio) and a spin–orbit splitting of 0.6 eV. To fit the Si  $2p_{3/2}$  spectra, each chemical state is represented by a Gaussian convoluted by a Lorentzian of 0.1 eV full width at half-maximum (fwhm). On the other hand, the C 1s spectra are simply reconstructed by sums of pure Gaussian components. In the least-squares fitting routine, we fix the Gaussian fwhm for each chemical state and in most cases BE positions are free parameters. The zero binding energy (the Fermi level, denoted  $E_F$ ) is taken at the leading edge of a clean metal surface (Ta) in electrical contact with the silicon crystal.

**C. C 1s NEXAFS.** C 1s NEXAFS spectra of the hydrocarbon films are recorded at different polar angles  $\theta$  between  $n$  (the

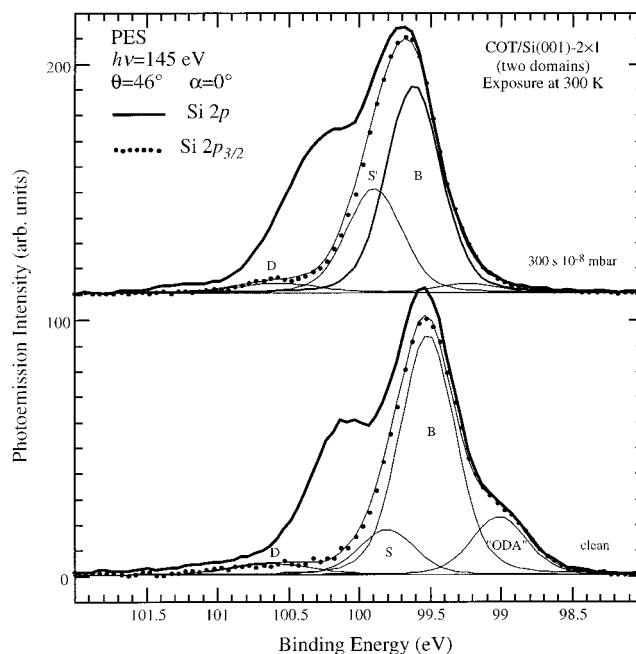


**Figure 3.** Si 2p core level photoemission spectra (thick solid line) and Si  $2p_{3/2}$  component, after  $2p_{1/2}$  stripping (dots), obtained from an “on-axis” Si(001) surface exposed to COT at 300 K (300 s,  $10^{-8}$  mbar). The curve is measured at  $\alpha = 0^\circ$  and  $\theta = 46^\circ$ . Fits of the Si  $2p_{3/2}$  spectra are also given (thin solid line). The Gaussian fwhm is 0.4 eV, for components “ODA”, B, S, and S’ and 0.55 eV for D (the Lorentzian fwhm is 0.1 eV for all components).

normal to the optical plane) and the electric field  $E$ ,<sup>25</sup> in the range of  $\sim 20^\circ$  (grazing incidence) to  $90^\circ$  (normal incidence). The special case of the vicinal surfaces needs some precisions (the geometry is given in Figure 2). In the “ortho” geometry,  $E$  is contained in a plane orthogonal to the  $\text{Si}_2$  dimer axis (aligned with the [110] axis). The angular scans are performed in the (110) silicon plane:  $\theta_{\text{ortho}}$  is the angle between the [001] axis and  $E$ . On the other hand, in the “para” geometry,  $E$  is contained in a plane parallel to the  $\text{Si}_2$  dimer axis. The scans are performed in the plane defined by  $n$  ( $n$  is inclined by  $5^\circ$  downstairs from [001]) and the [110] direction. Then  $\theta_{\text{para}}$  is the same as  $\theta$ , i.e., the angle between  $n$  and  $E$ .

For the chemisorbed film, the absorption curve is measured by collecting the partial electron yield (PEY): in order to increase the sensitivity to the adsorbate,<sup>26</sup> the head of the channeltron is biased to  $-250$  V. On the other hand, the absorption spectrum of the multilayer film is measured by collecting the total electron yield (TEY). The beamline transmission is obtained by measuring the TEY and PEY curves of a clean silicon surface. After normalization, the spectra are represented with an intensity jump, measured before the edge (at  $h\nu = 280$  eV) and far after the edge (at  $h\nu = 320$  eV), equal to one. The energy resolution of the light is about 500 meV. The photon energy is calibrated by subtracting the kinetic energy of Si 2p photoelectrons excited by first-order radiation ( $h\nu$ ) to that of Si 2p photoelectrons excited by second-order radiation ( $2h\nu$ ).

## III. Results and Discussion

**A. PES.** Core-level spectra are measured at normal emission ( $\alpha = 0^\circ$ ,  $\theta = 46^\circ$ ). The clean “on-axis” surface Si  $2p_{3/2}$  spectrum (Figure 3) can be fitted with four components. The pronounced surface core level at  $-0.53$  eV above bulk line B is assigned, in the framework of the asymmetric dimer, to half a monolayer (ML) of negatively charged outer dimer atoms (ODA; ref 24):



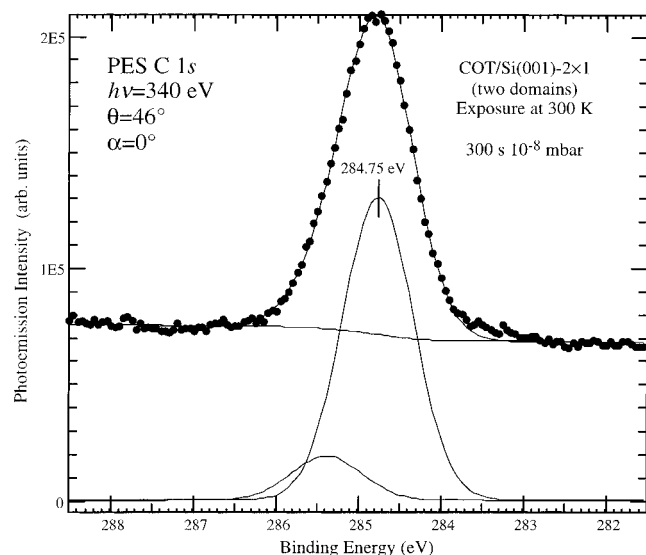


**Figure 4.** C 1s core-level photoemission spectrum (dots) of an “on-axis” Si(001) surface exposed to COT at 300 K (300 s,  $10^{-8}$  mbar). The curve is measured at  $\alpha = 0^\circ$  and  $\theta = 46^\circ$ . Its fit (solid line) by two Gaussians at 284.75 and 285.4 eV (fwhm = 1 eV) is also given.

its weight is 15% of the total spectral intensity. Calculations<sup>27</sup> and high-energy resolution spectra<sup>28</sup> suggest that the surface core level corresponding to the positively charged inner dimer is contained in the bulk line *B*. Line *S* (10% of the spectral weight), at about +0.3 eV from *B*, may be related to the second silicon atomic plane.<sup>28</sup> The fourth line (line *D*) situated at 1.1 eV from the line *B*, (about 4% of the total spectra intensity) needs to be introduced to take into account the asymmetry toward higher BE. Its origin is unclear.

For gas exposures longer than or equal to 300 s (under a nominal pressure of  $10^{-8}$  mbar), the Si 2p and C 1s core levels show that a saturation coverage is reached. In the Si 2p core-level spectrum (see Figure 3, exposure time of 300 s), the “surface state” (ODA) is now quenched, indicating a reaction of all of the silicon dimers with the molecule. The bulk line *B* itself has shifted to higher binding energy by +0.10 eV, in relation with a small change in surface band bending. The formation of Si–C bonds is reflected by the growth of a line *S'* (representing ~31% of the whole spectral weight, i.e., about 1 ML) introduced at +0.28 eV from *B*. High energy resolution PES data on surface core-level shifts induced by the chemisorption of various  $\pi$ -bonded molecules have been published recently. There is a great dispersion of the chemical shifts: for ethylene, the shift may be so small that there is not even any agreement about its direction, toward lower BE (–169 meV<sup>29</sup>) or toward higher BE (+128 meV<sup>30</sup>). On the other hand, larger BE shifts are observed for benzene (315 meV<sup>29</sup>) and for 1,4-cyclohexadiene (398 meV<sup>31</sup>), comparable to the one we find for COT.

The C 1s spectrum obtained after an exposure of 300 s (under  $10^{-8}$  mbar) is given in Figure 4. The spectrum is fitted by two Gaussians of fwhm equal to 1 eV each. The main peak (88% of the spectral weight) is found at 284.75 eV. Its companion shifted by 0.64 eV to higher binding energy simulates the slight asymmetry of the curve. Such a curve fitting cannot be interpreted in terms of two chemically distinct carbons, simply because the C 1s asymmetry can be due to a vibrational fine structure (for example, the energy of the C–H stretching mode in gas-phase ethylene is about 400 meV<sup>32</sup>).

**B. C 1s NEXAFS.** In Figure 5, we give the NEXAFS curves of the molecular solid (condensed on Si at 90 K) and of the

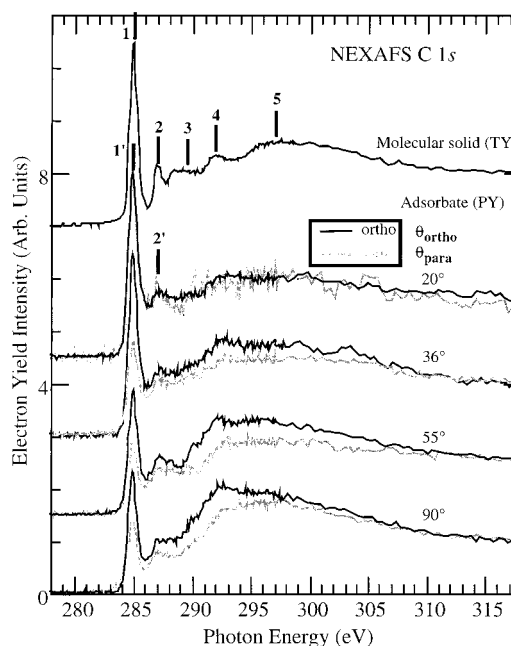


**Figure 5.** C 1s NEXAFS spectra of the molecular solid ( $10^{-8}$  mbar, 1400 s, 90 K) and of the chemisorbate on vicinal ( $5^\circ$ ) Si(001) ( $10^{-8}$  mbar, 300 s, 300 K). The NEXAFS polar scans are obtained in two azimuthal planes, one parallel (“para” geometry) and one orthogonal (“ortho” geometry) to the  $\text{Si}_2$  dimer axis.  $\theta_{\text{ortho}}$  ( $\theta_{\text{para}}$ ) is the angle between *E* and [001] (*n*; see Figure 2).

chemisorbed layer formed at 300 K (under a pressure of  $10^{-8}$  mbar, for 300 s) on a vicinal surface. In the latter case, NEXAFS measurements are made at saturation coverage, to minimize the contribution of species that may be adsorbed at step edges (see the discussion in section III.C).

Let us first concentrate on the molecular solid. The NEXAFS spectrum is nearly identical to that of COT on Pt(111), previously published by Hitchcock and co-workers.<sup>33</sup> We have noted no dichroic effect on the absorption intensity with varying radiation incidence; therefore, on Si, the molecules are randomly oriented (we give in Figure 5 the NEXAFS curve taken at  $\theta = 55^\circ$ ). Peaks 1 ( $h\nu = 285$  eV, of fwhm = 0.85 eV), 2 ( $h\nu = 287.1$  eV) and 3 ( $h\nu \sim 289.5$  eV) are attributed in ref 33 to transitions from C 1s to  $\pi^*$  molecular orbitals  $3a_2$ ,  $8e$ , and  $4b_1$ , respectively. (We note that a  $\text{CH}^*$  transition around 288 eV could well be concealed by the broad structure 3.) Features 4 ( $h\nu = 292$  eV) and 5 ( $h\nu \sim 297$  eV) are attributed to  $\sigma^*$  transitions, although peak 4 could be a shake up of the first  $\pi^*$  transition.<sup>34</sup>

The NEXAFS spectra of the chemisorbed layer displays a peak of clear  $\pi^*$  nature denoted 1' (at  $h\nu = 285$  eV, of fwhm = 0.85 eV), a second peak denoted 2' (at  $h\nu = 287.2$  eV) that seems to continue peak 2 of the molecular solid, and a third, broader transition at  $h\nu = 292$ – $293$  eV of  $\sigma^*$  character. The observation of a  $\pi^*$  transition shows that alkene groups survive after chemisorption of the molecule. These C=C groups should interact little with the substrate as peaks 1 and 1' have the same fwhm. The present NEXAFS results are therefore in agreement with the IR data of ref 17. Note that the “gap” between structures 1 and 2 of the molecular solid is now partly filled by new states related to the formation of silicon–carbon bonds.

In both azimuthal scanning planes, the “ortho” geometry and “para” geometry of Figure 2, the NEXAFS curves are dichroic. The  $\pi^*$  transition 1' ( $\sigma^*$  transition) is maximum for grazing (normal) incidence, and this suggests that most of the adsorbates lie rather “flat” on the surface. The angular dependence of peak

$2'$  is less clear. The absorption curves coincide for both azimuths in grazing geometry: this is not surprising as the direction of  $E$  is close to  $[001]$ . On the other hand, the intensity of the  $\pi^*$  transition ( $1'$ ) is larger at  $\theta_{\text{ortho}} = 90^\circ$  ( $E$  belongs to  $(001)$  and lies orthogonal to the  $\text{Si}_2$  dimer axis) than at  $\theta_{\text{para}} = 90^\circ$  ( $E$  lies parallel to the  $\text{Si}_2$  dimer axis). The ratio  $\pi^*(\theta_{\text{ortho}} = 90^\circ)/\pi^*(\theta_{\text{para}} = 90^\circ)$  is  $\sim 1.7$ . The latter observation is crucial in the discussion of the adduct geometries.

**C. Bonding Geometries.** Let us now inspect the various geometries given in Figure 1 and confront them to our NEXAFS data obtained on a vicinal surface. Let us have in mind that the intensity of the  $\text{C } 1s \rightarrow \pi^*$  NEXAFS transition is zero if  $E$  is orthogonal to the  $\pi$ -system. The spectra measured with  $E$  contained in the  $(001)$  plane, either parallel to the dimer axis ( $\theta_{\text{para}} = 90^\circ$ ) or perpendicular ( $\theta_{\text{ortho}} = 90^\circ$ ) give very interesting information.

Let us first consider the  $\pi$  system of “dual  $[2+2]$ ”, the geometry of the majority species according to Hovis and Hamers. The CC bond axes of the two alkene groups are parallel to the dimer row direction; therefore,  $E$  is orthogonal to the  $\pi$  system when it lies parallel to dimer row (i.e. perpendicular to the dimer axis) at  $\theta_{\text{ortho}} = 90^\circ$ . On the other hand,  $E$  is not orthogonal to the  $\pi$  system at  $\theta_{\text{para}} = 90^\circ$ .

In the “dual  $[4+2]$ ” geometry, the situation is reversed. The CC bond axes of the two alkene groups are parallel to the dimer axis; therefore,  $E$  is orthogonal to the  $\pi$  system at  $\theta_{\text{para}} = 90^\circ$ . Note that  $E$  is not orthogonal to the  $\pi$  system at  $\theta_{\text{ortho}} = 90^\circ$ .

It is easy to convince oneself, looking at Figure 1, that the  $p$  systems of “ $[2+2]$ ” (a conjugated triene) and “ $[4+2]$ ” (a conjugated diene) are perpendicular to planes which contain  $E$  when it lies parallel to the dimer axis, i.e., at  $\theta_{\text{para}} = 90^\circ$ .

Consequently, the observation of a nonvanishing  $\pi^*$  NEXAFS intensity at  $\theta_{\text{para}} = 90^\circ$  means that the “dual  $[2+2]$ ” geometry proposed by Hovis and Hamers should be present.

Conversely, a nonvanishing  $\pi^*$  intensity at  $\theta_{\text{ortho}} = 90^\circ$  signifies that “dual  $[2+2]$ ” is not the only adduct present on the surface. The other geometries of Figure 1, “dual  $[4+2]$ ”, “ $[2+2]$ ”, and “ $[4+2]$ ”, can account for this observation. Step edge adducts, if present, could also contribute to the  $\pi^*$  NEXAFS intensity at  $\theta_{\text{ortho}} = 90^\circ$ , as discussed below.

STM images<sup>35</sup> and adsorption studies<sup>36</sup> favor the bistep reconstruction proposed by Chadi.<sup>37</sup> Reactive sites distant by 3.85 Å (triply coordinated Si bearing one dangling bonds, buckled along the step direction) are present on the steps. For the vicinal surfaces, there is no general law concerning the respective reactivity of bistep and terrace sites vis-à-vis molecular species: water vapor dissociates preferentially on terrace sites<sup>38</sup> and “ethylene is chemisorbed on the terraces, not at steps”.<sup>1</sup> On the other hand,  $\text{H}_2$ , nonreactive with terrace dimers, breaks up on step dangling bond pairs.<sup>39</sup> Unfortunately, concerning the COT case, a detailed STM study of step reactivity was not given in ref 17, although the IR analysis has been made on a  $\text{Si}(001)$   $4^\circ$  vicinal surface. One of the four alkene groups of the COT molecule could make a cycloaddition reaction with a pair of step dangling bonds. For a vicinal surface cut off by  $5^\circ$  (present case), there is, on the average, a pair of step dangling bonds for seven  $\text{Si}_2$  dimers on a terrace (of width 31 Å). Therefore, step species could represent up to 22% of the surface species, if each terrace species occupies two adjacent dimer sites. If the step species is a conjugated triene similar to “ $[2+2]$ ”, it should contribute to the  $\pi^*$  NEXAFS intensity at  $\theta_{\text{ortho}} = 90^\circ$ . As indicated in section III.B., the ratio  $\pi^*(\theta_{\text{ortho}} = 90^\circ)/\pi^*(\theta_{\text{para}} = 90^\circ)$  is  $\sim 1.7$ . It seems very unlikely that bistep

species alone (at most 22% of the adsorbates) can contribute so much to the NEXAFS intensity in “ortho” geometry.

In addition to NEXAFS, PES give also information on the bonding geometry. As the “ $[2+2]$ ” and “ $[4+2]$ ” adducts of Figure 1 may prevent the reaction of the close neighbor  $\text{Si}_2$  site for steric hindrance reasons,<sup>40</sup> the presence of unreacted dimer states should be detected by Si 2p PES. This is not the case, as all Si 2p surface states are quenched. Therefore, “ $[2+2]$ ” and “ $[4+2]$ ” configurations seem unlikely, unless it is demonstrated that adsorption on sites adjacent to an already reacted site is not avoided. The latter two geometries appear as intermediate steps in the formation of the “dual  $[2+2]$ ” and “dual  $[4+2]$ ” bridging structures.

**D. Resonant Valence Band Photoemission.** Valence band spectroscopy performed at the photon energy of a given NEXAFS resonance is an interesting spectroscopic tool, as molecular orbitals of the adsorbate can be selectively involved in the decay process.<sup>41–44</sup> When a C 1s electron, lifted to an empty level, is sufficiently localized to the core-hole (such is the case for  $\pi^*$  transitions), two decay processes can be observed: (i) the decay involves two electrons of the valence band, with the excited electron remaining as a spectator, and (ii) the decay involves the promoted electron, termed in that case “participator”, and the final state is a one hole state (in the valence band), as in “regular” photoemission. In solid ethylene,<sup>41</sup> at  $h\nu$  corresponding to the C 1s  $\pi^*$  (lowest unoccupied molecular orbital) NEXAFS transition, the resonant one-hole channel is the highest occupied orbital (of  $\pi$  character). The situation is similar for solid benzene<sup>42</sup> and polystyrene.<sup>43</sup> The conditions leading to the resonance of a given MO is that it has a spatial extent around the core hole similar to that of the unoccupied orbital to which the C 1s electron is excited (for a discussion see ref 44).

Valence band spectra of a two-domain (“on-axis”) surface saturated by COT at 300 K are measured at grazing light incidence ( $\alpha = 26^\circ$ ,  $\theta = 20^\circ$ ), with photon energies around the C 1s edge. In Figure 6, we show the valence bands (normalized to equal photon flux) measured off-resonance (at  $h\nu = 282.6$  eV, curve a and b) and at the  $\pi^*$  resonance ( $h\nu = 285.15$  eV, curve c). Curve d (d results from the subtraction of the nonresonant contribution b to the resonant curve c) exhibits a strong participator line (denoted  $R$ ), superimposed on a stepped Auger-like spectrum. Line  $R$  is attributed to the free alkene  $\pi$  levels. This  $\pi$  band is centered at  $\sim 4$  eV below  $E_F$ , with a fwhm of  $\sim 2.6$  eV (the overall experimental resolution is  $\sim 0.59$  eV). Note that we have observed  $\pi$ -bond resonances at about the same BE for nonconjugated dienes that stick to the surface by one  $\text{C}=\text{C}$  group, leaving the other free.<sup>5,7</sup>

Coming back to the STM issue (refs 17–18), we note that at low bias ( $V_b = -1$  eV), the  $\pi$  band is too far from  $E_F$  to participate to the formation of the molecular image. So the reason two different footprints are observed in ref 18 remains unclear. On the other hand, given its width and position, the occupied  $\pi$  band is certainly involved in the tunneling process at high bias ( $-3 \text{ V} \leq V_b \leq -2.2 \text{ V}$ ). Because it is degenerate with bulk silicon bands (see Figure 6) the tunneling should be strongly enhanced. As in the two most probable models (“dual  $[4+2]$ ” and “dual  $[2+2]$ ”), the CC axis of the free alkene bonds are at right angle, and a careful examination of the size of molecular footprints, associated to image simulation, should permit an identification of the geometries, and a measurement of their statistical ratio.

#### IV. Conclusion

In this experiment, the adsorbed state of cyclooctatetraene on  $\text{Si}(001)\text{-}2\times 1$  is investigated. At saturation coverage, PES

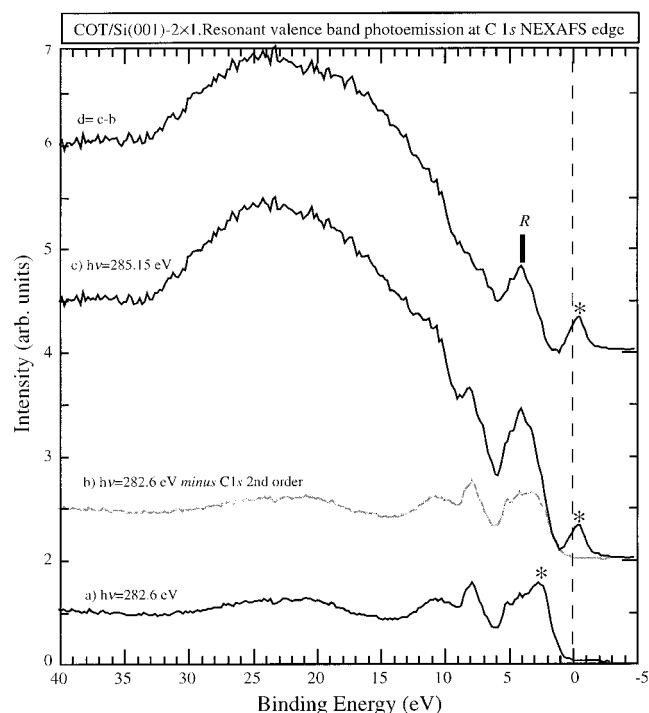


**Figure 6.** Valence band spectra of a Si(001) surface (two-domain) exposed to COT ( $10^{-8}$  mbar, 300 s, 300K), measured off-resonance (curve a) and on-resonance (curve c), at  $\theta = 20^\circ$  and  $\alpha = 26^\circ$ . The peak marked with an asterisk (\*) is the carbon 1s core level excited by second-order light. Curve b (in gray) is the off-resonance valence band to which the C 1s peak ( $2h\nu$ ) has been subtracted. Curve d is the resonant contribution, with **R** denoting the  $\pi$  level participant channel. Vertical scales are normalized with incident flux.

shows that all silicon dimer states are reacted. This observation is compatible with the bridge geometries proposed in the STM work by Hovis and Hamers (ref 17). For its part, C 1s NEXAFS spectroscopy shows that  $\pi$  bonds survive after chemisorption, confirming the IR data of ref 17. On the other hand, the angular study, performed on a single domain (vicinal) surface, indicates that the “dual [2+2]” adsorption geometry, proposed by Hovis and Hamers on the basis of STM images obtained at high substrate bias, cannot be the only species present on the surface. In fact, multiple adsorption geometries are adopted by the chemisorbed molecule. Finally, resonant valence band spectroscopy shows that a broad (2.6 eV wide) molecular  $\pi$  band is centered at  $\sim 4$  eV below  $E_F$ . This information may be useful for the interpretation/simulation of the STM images. As far as the bonding of COT on Si(001) is complex, the energetics of the various reaction pathways and final products of this antiaromatic molecule should deserve a careful computational study.

**Acknowledgment.** We thank Prof. P. Ballone for enlightening discussions and for communicating to us preliminary results of a density functional and molecular dynamics calculation concerning the reactivity of COT with Si(001)- $2\times 1$ . We are also very indebted to Prof. R. J. Hamers for reading the manuscript and giving us his comments on this work. Some of this work was supported by the French and Italian Ministries of Foreign Affairs (Program d’Actions Intégrées Franco-Italien Galilée 2000-2001).

## References and Notes

- (1) Yoshinobu, J.; Tsuda, H.; Onchi, M.; Nishijima, M. *J. Chem. Phys.* **1987**, *87*, 7332.
- (2) (a) Teplyakov, A. V.; Kong, M. J.; Bent, S. T. *J. Am. Chem. Soc.* **1997**, *119*, 1110. (b) Teplyakov, A. V.; Kong, M. J.; Bent, S. T. *J. Chem. Phys.* **1998**, *108*, 4599.
- (3) Hovis, J. S.; Liu, H.; Hamers, R. J. *J. Phys. Chem. B* **1998**, *102*, 6873.
- (4) Hovis, J. S.; Hamers, R. J. *J. Phys. Chem. B* **1997**, *101*, 9581.
- (5) Jolly, F.; Bournel, F.; Rochet, F.; Dufour, G.; Sirotti, F.; Taleb, A. *Phys. Rev. B* **1999**, *60*, 2930.
- (6) Hamaguchi, K.; Machida, S.; Mukai, K.; Yamashita, Y.; Yoshinobu, J. *Phys. Rev. B* **2000**, *62*, 7577.
- (7) Bournel, F.; Jolly, F.; Rochet, F.; Dufour, G.; Sirotti, F.; Torelli, P. *Phys. Rev. B* **2000**, *62*, 7645.
- (8) Gokhale, S.; Trischberger, P.; Menzel, D.; Widdra, W.; Dröge, H.; Steinrück, H.-P.; Birkenheuer, U.; Gutdeutsch, U.; Rösch, N. *J. Chem. Phys.* **1998**, *108*, 5554.
- (9) Wolkow, R. *Annu. Rev. Phys. Chem.* **1999**, *50*, 413.
- (10) Ault, A. J. *J. Chem. Educ.* **2000**, *77*, 57.
- (11) Andrés, J. L.; Castaño, O.; Morreale, A.; Palmeiro, P.; Gomperts, R. *J. Chem. Phys.* **1998**, *108*, 203.
- (12) Ballone, P. Unpublished results. Computations have been done using the density functional method and applying a recent approximation for the exchange energy (Perdew, J. P.; Burke, K.; Ernzerhof, M. *Phys. Rev. Lett.* **1996**, *77*, 3865; Errata: (E) **1997**, *73*, 1396). Kohn–Sham orbitals have been expanded on a basis of plane waves, and atomic coordinates have been optimized by the molecular dynamics method of Car and Parinello (Car, R.; Parinello, M. *Phys. Rev. Lett.* **1985**, *55*, 2471).
- (13) Dvorak, V.; Michl, J. *J. Am. Chem. Soc.* **1976**, *98*, 1080.
- (14) We use this notation for the reaction product despite the fact that the reaction pathway necessarily implies low-symmetry intermediates (see, e.g., for acetylene the calculation by Liu and Hoffmann. Liu, Q.; Hoffmann, R. *J. Am. Chem. Soc.* **1995**, *117*, 4082). We should rather speak of [2+2]-like final products.
- (15) Note that 1,5-cyclooctadiene, whose two alkene groups are separated by about the same distance, bonds only by one end (refs 4 and 5 of the present paper).
- (16) Using the notations single [4+2] and dual [4+2], one assumes implicitly that a planar intermediate species is formed. For the final products depicted in Figure 1, the term [4+2]-like should be less restrictive about the reaction pathways. As suggested by R. J. Hamers (private communication), when the  $D_{2d}$  molecular symmetry is conserved, these products could be equally formed by reaction of carbon atoms (4, 7) with one dimer, followed by reaction of carbons (3, 8) with another dimer. This would be a “radical” reaction.
- (17) Hovis, J. S.; Hamers, R. J. *J. Phys. Chem. B* **1998**, *102*, 687.
- (18) Padowitz, D. F.; Hamers, R. J. *J. Phys. Chem. B* **1998**, *102*, 8541.
- (19) Stöhr, J. *NEXAFS Spectroscopy*, Springer Series in Surface Sciences, Vol. 25; Springer-Verlag: Berlin, Heidelberg, New York, 1992.
- (20) Stöhr, J. *NEXAFS Spectroscopy*, Springer Series in Surface Sciences, Vol. 25; Springer-Verlag: Berlin, Heidelberg, New York, 1992; p 71.
- (21) An alternative strategy would consist in the use of very well oriented on-axis wafers (e.g., to  $\pm 0.1^\circ$ ) in order to create a “single domain” by electromigration. Nor is this method entirely satisfactory, as it leads to  $2\times 1$  and  $1\times 2$  domains in typical ratios 80:20 (Bullock, E. L.; Gunnella, R.; Pathey, L.; Abukawa, T.; Kono, S.; Natoli, C. R.; Johansson, L. S. O. *Phys. Rev. Lett.* **1995**, *74*, 2756).
- (22) Schwartzentruber, B. S.; Mo, Y.-W.; Webb, M. B.; Lagally, M. G. *J. Vac. Sci. Technol. A* **1989**, *7*, 2901.
- (23) Rochet, F.; Poncey, C.; Dufour, G.; Roulet, H.; Rodrigues, W. N.; Sauvage, M.; Bouliard, J. C.; Sirotti, F.; Panaccione, G. *Surf. Sci.* **1995**, *326*, 229.
- (24) Himpel, F. J.; Meyerson, B. S.; McFeely, F. R.; Morar, J. F.; Taleb-Ibrahimi, A.; Yarnoff, J. A. In *Proceedings of the Enrico Fermi School on “photoemission and Absorption spectroscopy of Solids and Interfaces with Synchrotron Radiation”*; Campagna, M.; Rosei, R., Eds.; North-Holland: Amsterdam, The Netherlands, 1990; p 203.
- (25) The polarization factor of the radiation is 100%, as the source is an undulator.
- (26) Stöhr, J. *NEXAFS Spectroscopy*, Springer Series in Surface Sciences, Vol. 25; Springer-Verlag: Berlin, Heidelberg, New York, 1992; p 151.
- (27) Pehlke, E.; Scheffler, M. *Phys. Rev. Lett.* **1993**, *71*, 2338.
- (28) Landemark, E.; Karlsson, C. J.; Chao, Y.-C.; Uhrberg, R. I. G. *Phys. Rev. Lett.* **1992**, *69*, 1588.
- (29) Fink, A.; Widdra, W.; Wurth, W.; Keller, C.; Stichler, M.; Achleitner, A.; Comelli, G.; Lizzit, S.; Baraldi, A.; Menzel, D. *Phys. Rev. B* In press.
- (30) Casaletto, M. P.; Zanon, R.; Carbone, M.; Piancastelli, M. N.; Aballe, L.; Weiss, K.; Horn, K. *Phys. Rev. B* **2000**, *62*, 17128.
- (31) Yamashita, Y.; Nagao, M.; Machida, S.; Hamaguchi, K.; Yasui, F.; Mukai, K.; Yoshinobu, J. *J. Electron Spectrosc. Relat. Phenom.* **2001**, *114–116*, 389.

- (32) Kempgens, B.; Köppel, H.; Kivimäki, A.; Neeb, M.; Cederbaum, L. S.; Bradshaw, A. M. *Phys. Rev. Lett.* **1997**, *79*, 3617.
- (33) Hitchcock, A. P.; Newbury, D. C.; Ishii, I.; Stöhr, J.; Horsley, J. A.; Redwing, R. D.; Johnson, A. L.; Sette, F. *J. Chem. Phys.* **1986**, *85*, 4849.
- (34) Stöhr, J. *NEXAFS Spectroscopy*, Springer Series in Surface Sciences, Vol. 25, 1992; p 260.
- (35) Griffith, J. E.; Kochanski, G. P.; Kubby, J. A.; Wierenga, P. E. *J. Vac. Sci. Technol. A* **1989**, *7*, 1914.
- (36) Dohnálek, Z.; Gao, Q.; Choyke, W. J.; Yates, J. T., Jr. *J. Chem. Phys.* **1995**, *102*, 2946.
- (37) Chadi, D. J. *Phys. Rev. Lett.* **1987**, *59*, 1691.
- (38) Chabal, Y. J.; Christman, S. B. *Phys. Rev. B* **1984**, *29*, 6974.
- (39) Dürr, M.; Hu, Z.; Biedermann, A.; Höfer, U.; Heiz, T. F. *Phys. Rev. B* **2001**, *63*, 121315(R).
- (40) As a matter of fact, the “[4+2]” geometry resembles the “butterfly” geometry of chemisorbed benzene, viewed as a [4+2] cycloaddition adduct, which leads to a saturation coverage of one molecule per two dimers (ref 8 of the present paper).
- (41) Wurth, W.; Menzel, D. *J. Electron Spectrosc. Relat. Phenom.* **1993**, *62*, 23.
- (42) Menzel, D.; Rocker, G.; Steinrück, H. P.; Coulman, D.; Heimann, P. A.; Huber, W.; Zebisch, P.; Lloyd, D. R. *J. Chem. Phys.* **1992**, *96*, 1724.
- (43) Kikuma, J.; Tonner, B. P. *J. Electron Spectrosc. Relat. Phenom.* **1996**, *82*, 41.
- (44) Gallet, J.-J.; Jolly, F.; Rochet, F.; Bournel, F.; Dufour, G.; Avila, P.; Sirotti, F.; Torelli, P. *J. Electron Spectrosc. Relat. Phenom.* **2002**, *122*, 11.